Controllable Clothoid Path Generation for Autonomous Vehicles

Songyi Zhang, Runsheng Wang, Zhiqiang Jian, Wei Zhan, *Member, IEEE*, Nanning Zheng, *Fellow, IEEE*, and Masayoshi Tomizuka, *Life Fellow, IEEE*

***Abstract*—This letter proposes a novel and simple smooth path generation algorithm for autonomous vehicles. The proposed method can rapidly generate feasible and curvature continuous paths connecting any two given states with null curvature. The generated path comprises straight lines, circular arcs and clothoid segments that are close to human driving behavior. Moreover, while keeping an accurate connection with the boundary states, the proposed method also allows fine-tuning the curve with the maximum curvature of the path and the midpoint's position, which makes it more flexible in avoiding obstacles while keeping feasibility. Various experiments show that the proposed method has extremely low time consumption and high robustness for different conditions. Meanwhile, it is more flexible than the recent research and the spline-based methods.**

***Index Terms*—Computational geometry, nonholonomic motion planning, wheeled robots.**

I. Introduction

With the increasing application of autonomous vehicles, more attention is paid to the vehicle's safety and comfort. As a basis for this demand, the local planning module is required to rapidly generate a smooth path to guide the vehicle to a specific pose while avoiding environmental obstacles.

A smooth path is required to be at least curvature continuity (G^2-continuity). According to the nonholonomic constraints of the vehicle, sudden changes in orientation are not allowed. Meanwhile, the curvature of the path should not exceed the given boundary. Moreover, the front wheel angle of the vehicle, associated with the curvature of the path, cannot suddenly change either. Therefore, except for a few low-speed scenes, the generated path should also have a continuous curvature profile to avoid slowing the vehicle down to trace the sudden curvature changes.

The widely used G^2-continuity path generation methods include quintic splines, high-order Bézier curves, clothoids, etc. The quintic splines and Bézier curves can be easily solved or modified with the boundary conditions or control points, which makes them easily integrated with the optimization methods. However, these two curves make no promise on the maximum curvature and the curvature change rate, which may lead to kinetically infeasible solutions.

The clothoid-based path can overcome the curvature issue. The clothoid is a curve whose curvature changes linearly along the arc length, allowing us to control each point's curvature by adjusting the curve length and curvature at two boundaries. This characteristic allows us to use clothoids (with their degraded form, the circular arcs and the straight line segments) to form a G^2-continuous complex path with controllable curvature. Therefore, its curvature is fully controllable for a curve of multiple clothoids. Moreover, the constant curvature change rate leads to a uniform rotation of the front wheel, which is close to human driving behavior. The abovementioned advantages make clothoid competitive in the planning application. However, different from the spline-based curves, the position of a clothoid has a complex relationship to its curvature. Thus, it cannot be easily solved with boundary conditions of control points.

The clothoid trigonometry proposed by Walton et al. [1] simplifies the process of solving clothoid-based paths under boundary constraints. The path proposed by Walton et al. is composed of two clothoids with a circular arc together. With their rigorous analysis, such a curve can smoothly connect two states with null curvature, while the shape of the curve can be uniquely determined with the two states and the maximum curvature. However, their method fails to achieve an efficient solution for some of the boundary constraints. For the simplest symmetric case (two clothoids are identical), Wilde et al. [2] proposed a simple and fast method to solve the parameters. As a comparison, fewer studies focus on unsymmetric cases. In Gim et al.'s method [3], the unsymmetric problem is solved with a bisection method, but it still cannot meet the high speed and robustness requirement for planning. Moreover, in most planning and map editing scenarios, the fine-tuning of the curve should also consider the positional constraints, while the existing methods only consider the curvature.

To overcome the abovementioned problems, this letter proposes a novel, simple and elegant method to construct clothoid based G^2-continuous curve between any boundary states with null curvature. The simplified calculations make the proposed method more efficient and robust than existing methods. Moreover, to our best knowledge, apart from fine-tuning the curve with the maximum curvature, the proposed method is the first work that also allows tuning with the position of the midpoint of the curve, which provides higher flexibility for local planning and HD map editing usage.

Manuscript received 18 March 2023; accepted 8 June 2023. Date of publication 22 June 2023; date of current version 12 July 2023. This letter was recommended for publication by Associate Editor P. Gao and Editor A. Bera upon evaluation of the reviewers' comments. This work was supported by the National Natural Science Foundation of China under Grants 62088102 and 61790563. *(Corresponding author: Nanning Zheng.)*

Songyi Zhang, Runsheng Wang, Zhiqiang Jian, and Nanning Zheng are with the Institute of Artificial Intelligence and Robotics, Xi'an Jiaotong University, Xi'an, Shaanxi 710049, China (e-mail: zhangsongyi@stu.xjtu.edu.cn; wrs666@stu.xjtu.edu.cn; flztiii@stu.xjtu.edu.cn; nnzheng@mail.xjtu.edu.cn).

Wei Zhan and Masayoshi Tomizuka are with the Department of Mechanical Engineering, University of California, Berkeley, CA 94720-1740 USA (e-mail: zhanwei0102@gmail.com; tomizuka@me.berkeley.edu).

This letter has supplementary downloadable material available at https://doi.org/10.1109/LRA.2023.3288761, provided by the authors.

Digital Object Identifier 10.1109/LRA.2023.3288761

Various experiments are carried out with randomly generated boundary conditions. Compared with recent research and the spline-based methods, the proposed method performs better in both calculation speed and flexibility.

II. Related Work

According to the linearized curvature profile, the clothoid is widely used in local planning applications. Specifically, the usage of clothoid can be divided into two types, individually and grouped, respectively. Due to the complexity of position calculation with the clothoid, the individually used case always generates an open-loop clothoid solution and uses it as the motion primitive, then the whole path is generated with search-based approaches. For instance, Zhang et al. [4] and Pang et al. [5] combine the clothoid with the hybrid A* method to find a smooth path in complex scenarios. However, the search-based approach cannot achieve the exact connection between two states.

Compared with individual clothoid, composite dual clothoid (a.k.a. elementary path) are easier to control. The parameters of the clothoids can be solved with the boundary poses. According to whether the two clothoids are identical, the elementary path can be divided into symmetric and unsymmetric cases. Wilde et al. [2] proposes a closed-form expression to find the accurate solution for the symmetric cases. For unsymmetric cases, an iterative-based approach is necessary. For instance, Gim et al. [3] introduce a bisection method to find a feasible solution. However, their algorithm is still too complex to meet the real-time computing requirement of local planning.

Bending circular arcs into elementary paths allows us to fine-tune the shape of the curve while meeting the curvature requirement. For the symmetric elementary path, Wilde et al. [2] solve the length of the circular arc with Newton's method. Then, Kiss et al. [6] further consider the influence of different circular arcs. However, such an approach cannot be extended to unsymmetric cases. The symmetric elementary path with circular arcs can also represent in concentric circles form, which is firstly introduced in Fraichard's work [7] to smooth Reeds Shepp's path. Again, Fraichard's method only works with symmetric cases, while the shape of the curve cannot be easily modified. Compared with the abovementioned methods, the proposed method provides also provides the solution for unsymmetric cases. Moreover, position-based fine-tuning can better accomplish the adjustment of the curve.

The elementary path is widely adopted in planning on structured roads. For instance, Funker et al. [8] use it to generate the reference path for turning. Silva et al. [9] and Tian et al. [10] use two elementary paths to perform smooth lane changes. Multiple elementary paths are also used in longer global path generation. Gim et al. [11] and Bertolazzi et al. [12] generate a long smooth path with waypoints, and Lambert et al. [13] optimize such paths to avoid the obstacles. These applications also share the benefits of the improvements in the proposed elementary path calculation.

Besides the planning usage, another application area for clothoid is road design and HD-map generation. Due to the controllable curvature profile, the clothoids have already been adopted in highway design to connect straight and arc parts [14]. To design such a path, it's important to have the flexibility to fine-tune each part individually. This is achieved by Walton et al. [1] with the clothoid spline, which is composed of multiple elementary paths. However, the calculations are still too complicated, and the curve can only be tuned with maximum curvature. HD maps like OpenDrive also adopt clothoid as a component to describe the shape of a road [15], and can be generated with real-world data. For instance, Zhou et al. [16] model the shape of highways with multiple symmetric elementary paths. It is still required for the curve to be fine-tuned with the position to fit the existing data better. Compared with the existing algorithms, the proposed method is easier to realize the abovementioned requirements.

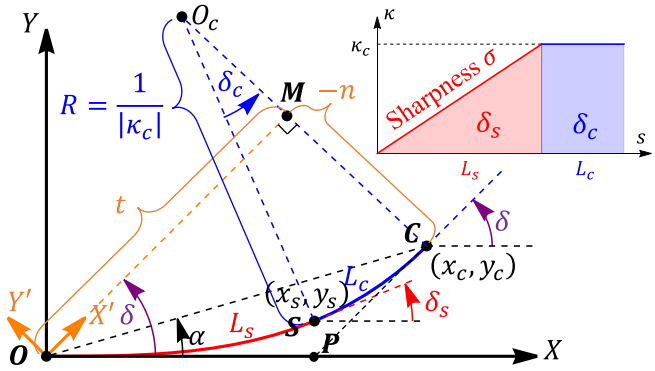

Fig. 1. Clothoid-arc segment and its curvature profile. The clothoid part is shown in red, while the circular arc part is shown in blue.

III. Primitive Clothoid-Arc Segment

This letter aims to find a feasible G^2-continuous path composed of straight lines, circular arcs, and clothoids to connect two states with null curvatures. Inspired by [2], before analyzing the whole complex problem, we first investigate the primitive clothoid-arc segment as the basic element. The clothoid-arc segment is constructed with clothoid and circular arc parts. The curvature of the clothoid variates linearly along its station, from 0 to κ_c. Under the G^2-continuous constraint, the curvature of the circular arc is constantly κ_c. Such a composed curve is called a clothoid-arc segment, shown as Fig. 1.

Without the loss of generality, we can assume the clothoid-arc segment starts from the origin $\mathbf{O}$ while having the same orientation as the x-axis to analyze its shape properties. Assuming the clothoid part with length L_s ends at $\mathbf{S} = (x_s, y_s)$, meanwhile, the circular arc part with length L_c and curvature κ_c ends at $\mathbf{C} = (x_c, y_c)$, and the heading of the curve at $\mathbf{S}$ and $\mathbf{C}$ are δ_s and δ, respectively. Furthermore, the orientation increment of the circular arc part δ_c can be calculated as $\delta_c = \delta - \delta_s$, and the curvature change rate σ of the clothoid part can be calculated as $\sigma = \kappa_c / L_s$. The clothoid ratio $\lambda \triangleq \delta_s / \delta$, $\lambda \in [0, 1]$ is introduced to simplify the expression, where $\delta_s = \lambda\delta$, $\delta_c = (1 - \lambda)\delta$. The degenerate case $\lambda = 0, 1$ means the curve is completely circular arc or clothoid, respectively.

The abovementioned variables $\delta, \delta_s, \delta_c, \kappa_c, \sigma, \lambda, L_s$ and L_c fully define the shape of the clothoid segment. Except for the always positive variables L_s, L_c and λ, other variables have the same sign, where positive variables correspond to the left turns and vice versa. However, these variables can be simplified since they are not independent. Besides the explicitly mentioned ones,

the curvature profile gives

$$L_s = \frac{2\delta_s}{\kappa_c},\ L_c = \frac{\delta_c}{\kappa_c}. \tag{1}$$

The basic relationships between these variables allow us uniquely determined the shape of the curve with any 3 independent ones among them, like $\{\kappa_c, L_s, L_c\}$ or $\{\delta, \lambda, \sigma\}$. They are the open-loop representation for the curve since no additional constraints are applied to the terminal point.

Once the shape of the curve is determined, the positions of its terminal points can be calculated as

$$x_c = x_s + \frac{\sin(\delta) - \sin(\lambda\delta)}{\kappa_c},\ y_c = y_s + \frac{\cos(\lambda\delta) - \cos(\delta)}{\kappa_c},$$
$$x_s = \frac{2\lambda\delta}{\kappa_c}\frac{1}{\eta}\mathcal{C}(\eta),\ y_s = \frac{2\lambda\delta}{\kappa_c}\frac{1}{\eta}\mathrm{sgn}(\delta)\mathcal{S}(\eta),$$

where $\mathcal{S}$ and $\mathcal{C}$ are Fresnel integrals [17] with $\eta \triangleq \sqrt{\frac{\lambda|\delta|}{\pi/2}}$.

Inspired by [2], a $\delta-$rotated coordinate system $X'OY'$ can be used to simplify the calculation. In $X'OY'$, (x_c, y_c) is transformed into the new coordinates (t, n), where

$$\begin{aligned} t &\triangleq x_c\cos\delta + y_c\sin\delta \\ &= x_s\cos\delta + y_s\sin\delta + \frac{1}{\kappa_c}\sin[(1-\lambda)\delta] \end{aligned} \tag{2a}$$

$$\begin{aligned} n &\triangleq -x_c\sin\delta + y_c\cos\delta \\ &= -x_s\sin\delta + y_s\cos\delta - \frac{1}{\kappa_c}\{1-\cos[(1-\lambda)\delta]\}. \end{aligned} \tag{2b}$$

The relationship of (t, n) with other parameters is shown in the orange elements in Fig. 1, where $\mathbf{M}$ is the footprint of $\mathbf{C}$ on the x'-axis. For any clothoid-arc segment, t is always positive, while n has an opposite sign with δ. Therefore, in Fig. 1, $-n$ is used as the notation instead.

According to [2], using (t, n) instead of (x_c, y_c) is more conducive to the related problems. This is because the edge $\overline{\mathbf{OM}}$, $\overline{\mathbf{MC}}$ and the clothoid-arc segment $\widehat{\mathbf{OC}}$ can form a triangle-liked structure, and the problems can be solved with trigonometry-liked methods.

The (2) can be rewritten into

$$t = \frac{1}{\kappa_c}\cos_{\mathcal{E}}(\delta;\lambda),\ n = -\frac{1}{\kappa_c}\sin_{\mathcal{E}}(\delta;\lambda), \tag{3}$$

where $\cos_{\mathcal{E}}$ and $\sin_{\mathcal{E}}$ are

$$\cos_{\mathcal{E}}(\delta;\lambda) \triangleq 2\lambda\delta\cos_{\mathcal{C}}(\delta;\lambda) + \sin[(1-\lambda)\delta],$$
$$\sin_{\mathcal{E}}(\delta;\lambda) \triangleq 2\lambda\delta\sin_{\mathcal{C}}(\delta;\lambda) + 1 - \cos[(1-\lambda)\delta],$$

while $\cos_{\mathcal{C}}$ and $\sin_{\mathcal{C}}$ are

$$\cos_{\mathcal{C}}(\delta;\lambda) \triangleq \begin{cases} \frac{1}{\eta}\begin{pmatrix}\cos\delta\\ \sin\delta\end{pmatrix}^{\mathsf{T}}\begin{pmatrix}\mathcal{C}(\eta)\\ \mathrm{sgn}(\delta)\mathcal{S}(\eta)\end{pmatrix} & \eta \neq 0 \\ \cos\delta & \eta = 0 \end{cases}, \tag{4a}$$

$$\sin_{\mathcal{C}}(\delta;\lambda) \triangleq \begin{cases} \frac{1}{\eta}\begin{pmatrix}\sin\delta\\ -\cos\delta\end{pmatrix}^{\mathsf{T}}\begin{pmatrix}\mathcal{C}(\eta)\\ \mathrm{sgn}(\delta)\mathcal{S}(\eta)\end{pmatrix} & \eta \neq 0 \\ \sin\delta & \eta = 0 \end{cases} \tag{4b}$$

It is worth noting that (4) is the general form of the corresponding expression in [2]. When $\lambda = 1$ (pure clothoid segment), (4) will degenerate to that in [2]. Meanwhile, it is necessary to claim that $\sin_{\mathcal{C}}(\delta;\lambda)$ is defined negative to that in [2]. This is because when $\lambda = 0$, $\sin_{\mathcal{C}}(\delta;\lambda)$ can be degenerate to $\sin\delta$ instead of $-\sin\delta$.

The functions $\cos_{\mathcal{E}}$ and $\sin_{\mathcal{E}}$ have excellent differential properties. With

$$\frac{\partial}{\partial\delta}\cos_{\mathcal{E}}(\delta;\lambda) = -\sin_{\mathcal{E}}(\delta;\lambda) + 1 + \lambda\cos_{\mathcal{C}}(\delta;\lambda), \tag{5a}$$

$$\frac{\partial}{\partial\delta}\sin_{\mathcal{E}}(\delta;\lambda) = \cos_{\mathcal{E}}(\delta;\lambda) + \lambda\sin_{\mathcal{C}}(\delta;\lambda), \tag{5b}$$

$$\frac{\partial}{\partial\lambda}\cos_{\mathcal{E}}(\delta;\lambda) = \delta\cos_{\mathcal{C}}(\delta;\lambda), \tag{5c}$$

$$\frac{\partial}{\partial\lambda}\sin_{\mathcal{E}}(\delta;\lambda) = \delta\sin_{\mathcal{C}}(\delta;\lambda), \tag{5d}$$

the derivatives of these functions can be simply calculated.

Next, as an auxiliary definition, the angle between $\overline{\mathbf{OC}}$ and the x-axis is noted as α, which has the same sign as δ. According to Fig. 1, α meets the equation

$$\tan(\delta-\alpha) = \tan_{\mathcal{E}}(\delta;\lambda) \triangleq \frac{\sin_{\mathcal{E}}(\delta;\lambda)}{\cos_{\mathcal{E}}(\delta;\lambda)}. \tag{6}$$

IV. Solution of the Clothoid-Arc Segment

Considering the inconvenience of the open-loop representation mentioned in Section III, this section aims to solve the shape variables of a clothoid-arc segment based on different boundary conditions. According to the degree of freedom of the system, 3 individual boundary constraints are required. Meanwhile, in most applications for non-holonomic vehicles, the boundary constraints must include δ, which represents the difference from the current orientation of the vehicle to the target one. If the boundary conditions are $\{\delta, t, \lambda\}$, there are still closed-form solutions. According to (1) and (3), the rest of the parameters can be calculated as

$$L_s = \lambda\frac{2\delta\, t}{\cos_{\mathcal{E}}(\delta;\lambda)},\qquad L_c = \frac{1-\lambda}{2}\frac{2\delta\, t}{\cos_{\mathcal{E}}(\delta;\lambda)}, \tag{7a}$$

$$\kappa_c = \frac{1}{t}\cos_{\mathcal{E}}(\delta;\lambda),\qquad n = -t\,\tan_{\mathcal{E}}(\delta;\lambda). \tag{7b}$$

For the other combination of boundary conditions, one can first find the corresponding t and λ, and then finish the calculation with (7). Three typical boundary conditions are investigated, which are $\{\delta, t, \kappa_c\}$, $\{\delta, t, n\}$, and $\{\delta, x_c, y_c\}$, respectively. Since $\{\delta, x_c, y_c\}$ can be transformed to $\{\delta, t, n\}$, only the first two cases are considered. According to (7b), the solution on λ for these cases leads to

$$\lambda = \cos_{\mathcal{E}}^{-1}(\delta; t\,\kappa_c),\ \lambda = \tan_{\mathcal{E}}^{-1}\left(\delta; -\frac{n}{t}\right), \tag{8}$$

where $\cos_{\mathcal{E}}^{-1}$ and $\tan_{\mathcal{E}}^{-1}$ are the inverse function on λ of $\cos_{\mathcal{E}}$ and $\tan_{\mathcal{E}}$ when δ is given. Such inverse functions can be simply solved by Newton's method with (5c) and (5d). For any initial λ within [0,1], the residual on λ will converge to 10^{-3} in 1 to 2 iterations.

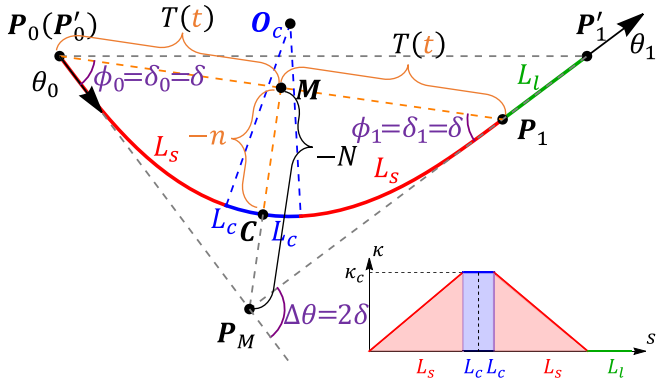

Fig. 2. A symmetric elementary path and its curvature profile.

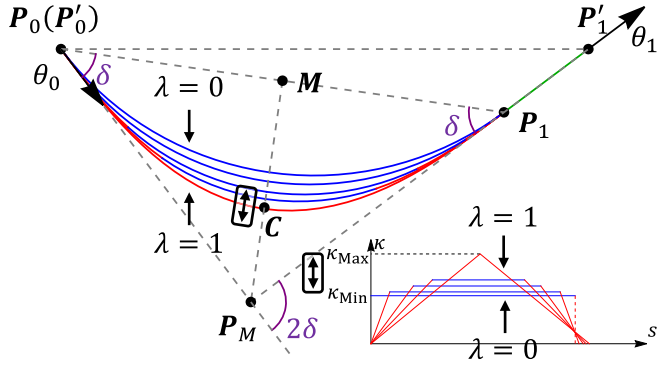

Fig. 3. Different symmetric elementary paths in the same enveloping triangle with multiple tuning methods presented.

V. Elementary Path

The clothoid-arc segment is a helpful tool to solve the original interpolation problem between two states with null curvature. Because of the non-zero curvature at the terminal point, the clothoid-arc segment must be present in pairs in the interpolated curve. In each pair, two clothoid-arc segments with the same κ_c are smoothly connected at their terminal point. Such a clothoid-arc segment pair is called an elementary path or a CC-turn.

This section considers the solution for connecting boundary states with a single elementary path. The initial and terminal states are noted as $\mathbf{P}_0$ and $\mathbf{P}_1$, meanwhile, they have the orientation θ_0 and θ_1, respectively. Moreover, the orientation change of the boundary states is defined as $\Delta\theta \triangleq \theta_1 - \theta_0 \in [-2\pi, 2\pi]$. Similar to that in the clothoid-arc segment, positive and negative $\Delta\theta$ means left and right turn, respectively.

Before conducting a detailed analysis, it is important to claim that the boundary conditions cannot be arbitrarily selected. Considering the degenerate form at $\lambda = 0$, where the elementary path turns into an arc segment (An inferior arc for $|\Delta\theta| \leq \pi$ and a superior arc for the rest of cases). Then, $\overrightarrow{\mathbf{P}_0\mathbf{P}_1}$ is the chord of such arc, meanwhile θ_0 and θ_1 are the tangent direction at $\mathbf{P}_0$ and $\mathbf{P}_1$, respectively. Therefore, it can be proved that θ_0 and θ_1 lay in the different half plane split by $\overrightarrow{\mathbf{P}_0\mathbf{P}_1}$. This is also the necessary condition for the existence of a single elementary path solution.

When $|\Delta\theta| \leq \pi$, the ray $\{\mathbf{P}_0, \theta_0\}$ and $\{\mathbf{P}_1, \theta_1 + \pi\}$ must intersect at a point, notated as $\mathbf{P}_M$, shown in Fig. 2. The triangle $\triangle\mathbf{P}_0\mathbf{P}_M\mathbf{P}_1$ is then called the enveloping triangle since the whole elementary path is contained in it. Such the enveloping triangle can be determined with $\{T, \delta, \Delta\phi\}$ without regard to the influence of absolute position and orientation, where

$$T \triangleq \frac{\|\mathbf{P}_0\mathbf{P}_1\|}{2},\ \delta \triangleq \frac{\Delta\theta}{2},\ \Delta\phi = \frac{\phi_0 - \phi_1}{2},$$

and ϕ_0 and ϕ_1 are the bottom corners' angles of $\triangle\mathbf{P}_0\mathbf{P}_M\mathbf{P}_1$, meanwhile having the same sign with δ and $\Delta\theta$. According to the trigonometry rules, $\phi_0 + \phi_1 = 2\delta$ holds. Several other notations for the enveloping triangle are introduced as follows. The middle point of $\mathbf{P}_0$ and $\mathbf{P}_1$ is noted as $\mathbf{M}$, while the directed length of $\overrightarrow{\mathbf{P}_M\mathbf{M}}$ is noted as N, having the opposite sign with $\Delta\theta$ for $|\Delta\theta| < \pi$, and same sign for $|\Delta\theta| > \pi$. Next, the subscript 0 and 1 are appended to distinguish the variables of the two clothoid-arc segments, like δ_0 and δ_1, n_0 and n_1, etc. The abovementioned symbols are partially illustrated in Fig. 2.

Finally, it is worth noting that all the deductions in the following parts are under the condition $|\Delta\theta| \leq \pi$. However, expect specified ones, these conclusions also hold for $|\Delta\theta| > \pi$, even though the "enveloping" triangle is conducted with the intersection of the ray $\{\mathbf{P}_0, \theta_0 + \pi\}$ and $\{\mathbf{P}_1, \theta_1\}$, and does not contain the elementary path completely.

The following analysis is split into two categories with the relationship between two clothoid-arc segments. In the first category, the two segments have the same parameters. Meanwhile, the second category contains the general rest situations. These two categories are called symmetric and unsymmetric elementary paths and will be analyzed in the following parts.

A. Symmetry Elementary Path

This part considers the generation of a symmetric elementary path in an enveloping triangle. According to the symmetry, the enveloping triangle is required to be isosceles, where $\Delta\phi = 0$. Introducing an extra straight-line segment can extend its adaptability. As shown in Fig. 2, for a non-isosceles triangle $\triangle\mathbf{P}_0'\mathbf{P}_M\mathbf{P}_1'$ with $\|\mathbf{P}_0'\mathbf{P}_M\| < \|\mathbf{P}_M\mathbf{P}_1'\|$, shown in Fig. 2, one can first calculate the length difference $L_l = \|\mathbf{P}_M\mathbf{P}_1'\| - \|\mathbf{P}_0'\mathbf{P}_M\|$, and then find point $\mathbf{P}_1$ on $\mathbf{P}_M\mathbf{P}_1'$ where $\mathbf{P}_1\mathbf{P}_1' = L_l$. Then, $\triangle\mathbf{P}_0'\mathbf{P}_M\mathbf{P}_1$ will be an isosceles triangle. The whole generated path is then composed of an elementary path in $\triangle\mathbf{P}_0'\mathbf{P}_M\mathbf{P}_1$ and a following straight line segment with length L_l. In the following part, only the elementary path generation in an isosceles triangle is considered since generating isosceles triangles is a fixed preprocessing step for general cases.

The solution of the symmetry elementary path is simple, where the parameters are $\delta_0 = \delta_1 = \delta$ and $t_0 = t_1 = T$. Then, the rest parameters can be deduced with (7).

According to (8), for a fixed isosceles triangle, there are three methods to tune the shape of the elementary path, which are tuning λ, κ_c and n, respectively. The effects of tuning these parameters are shown in Fig. 3.

The effects of tuning λ are first considered. λ can choose freely between 0 to 1. According to (7b), larger λ corresponds to larger $|n|$. This means the elementary path will move away from the line $\mathbf{P}_0\mathbf{P}_1$ while λ increases. Meanwhile, when $|\Delta\theta| \leq \pi$, the larger λ represents higher $|\kappa_c|$ and lower $|\sigma|$.

Compared with tuning λ directly, tuning κ_c and n with (8) are more natural, easy-to-use choices. As for κ_c, an example is to control the curvature of the curve lower than a specific curvature limit $\kappa_{\max}$. Thus, the generated curve can be traced with a curvature-limited vehicle. The corresponding maximum $\lambda_{\max}$ can be solved with (8).

Finally, solving parameters by n gives us a new, convenient way to tune the shape of the elementary path. This could also be achieved by tuning the position of midpoint $\mathbf{C}$ along the midline $\overline{\mathbf{MP}_M}$, which provides a friendly elementary path editing user interface. For instance, one can first pick $\mathbf{C}$ as the intersection between $\overline{\mathbf{MP}_M}$ and the target object (the boundary of the obstacles or the reference path), then the generated curve is guaranteed to pass through $\mathbf{C}$.

Apart from using (8) directly in the algorithm, we can also use the midline ratio $\eta_n \triangleq n/N$ as the given constraint. According to (7b)

$$\eta_n \triangleq \frac{n}{N} = -\frac{1}{N}\frac{-N}{\tan\delta}\tan_{\mathcal{E}}(\delta;\lambda) = \frac{\tan_{\mathcal{E}}(\delta;\lambda)}{\tan\delta}, \tag{9}$$

which leads to the solution

$$\lambda = \tan_{\mathcal{E}}^{-1}(\delta, \eta_n \tan\delta)$$

B. Unsymmetric Elementary Path

The more general cases are considered in this part. As a simplification, we can assume $\lambda_0 = \lambda_1 = \lambda$. Otherwise, if $\lambda_0 \neq \lambda_1$, an equivalent problem can be formed by re-selecting the connection point $\mathbf{C}$.

Since the two segments share the same parameters κ_c and λ, the primary differences between them are δ_0 and δ_1, respectively. An auxiliary variable $\Delta\delta$ is introduced as $\Delta\delta \triangleq (\delta_0 - \delta_1)/2$. Furthermore, since $\delta_0 + \delta_1 = 2\delta$, δ_0 and δ_1 can be equivalent represented by δ and $\Delta\delta$.

Next, the limitation of the unsymmetric elementary path is considered. Unlike the symmetric one, the unsymmetric elementary path no longer requires the enveloping triangle to be isosceles. However, this does not mean an unsymmetric elementary path can be formed for any enveloping triangle. The degraded case of such a problem is the elementary path only consists of a single clothoid-arc segment, while the other one's length is reduced to 0. In such a case, the enveloping triangle $\triangle\mathbf{P}_0\mathbf{P}_M\mathbf{P}_1$ turns into $\triangle\mathbf{OPC}$ in Fig. 1, resulting as $\alpha_0 = \phi_0$ and $\delta_0 = \Delta\theta = 2\delta$ by their correspondence. Note that the subscripts 0 for α and δ indicate that they are the parameter of the first clothoid-arc segment. According to (6),

$$\begin{aligned}&\tan(\delta - \Delta\phi) = \tan(2\delta - \phi_0)\\ &= \tan(\delta_0 - \alpha_0) = \tan_{\mathcal{E}}(\delta_0, \lambda) = \tan_{\mathcal{E}}(2\delta, \lambda).\end{aligned}$$

Therefore the conditions for the enveloping triangle lead to

$$|\Delta\phi| \leq |\delta - \tan^{-1}[\tan_{\mathcal{E}}(2\delta, \lambda)]|. \tag{10}$$

When $\lambda = 1$, an approximate form of (10) is $|\Delta\phi| \leq |\delta|/3$.

When $\Delta\phi$ does not meet (10), a similar pre-processing approach can be performed like that to the symmetric case, where a predecessor or successor straight line segment is used to modify the enveloping triangle. Similarly, since the pre-processing step is definite, we can assume the enveloping triangle must satisfy (10).

The relationship between these variables can be deduced with trigonometric operations. According to Fig. 4, the auxiliary

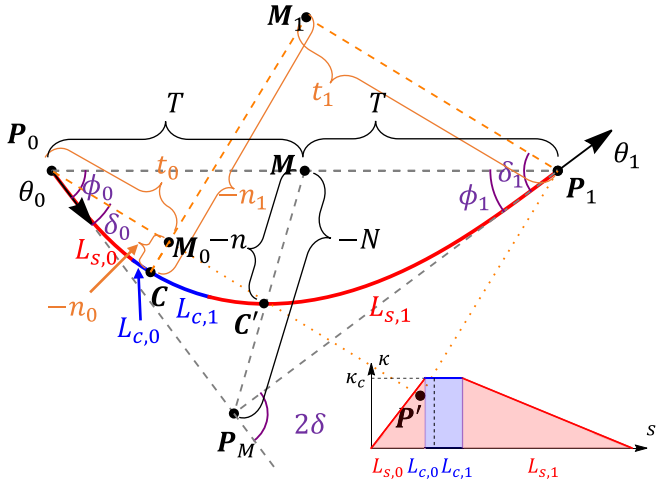

Fig. 4. An unsymmetric elementary path and its curvature profile.

lines $\overline{\mathbf{P}_0\mathbf{M}_0}$, $\overline{\mathbf{M}_0\mathbf{C}}$ and $\overline{\mathbf{P}_1\mathbf{M}_1}$ and $\overline{\mathbf{M}_1\mathbf{C}}$ are conducted for both segments, and a right triangle $\triangle\mathbf{P}_0\mathbf{P}'\mathbf{P}_1$ can be built by paralleled edges.

The trigonometry in $\triangle\mathbf{P}_0\mathbf{P}'\mathbf{P}_1$ leads to

$$t_1 + t_0 = \frac{2}{\kappa_c}\overline{\mathfrak{C}}(\delta, \Delta\delta; \lambda) = 2T\cos(\Delta\delta - \Delta\phi), \tag{11a}$$

$$n_1 - n_0 = \frac{2}{\kappa_c}\Delta\mathfrak{S}(\delta, \Delta\delta; \lambda) = 2T\sin(\Delta\delta - \Delta\phi), \tag{11b}$$

where

$$\overline{\mathfrak{C}}(\delta, \Delta\delta; \lambda) \triangleq \frac{\cos_{\mathcal{E}}(\delta+\Delta\delta;\lambda) + \cos_{\mathcal{E}}(\delta-\Delta\delta;\lambda)}{2}$$

$$\Delta\mathfrak{S}(\delta, \Delta\delta; \lambda) \triangleq \frac{\sin_{\mathcal{E}}(\delta+\Delta\delta;\lambda) - \sin_{\mathcal{E}}(\delta-\Delta\delta;\lambda)}{2}$$

Equation (11) can be represented as

$$\sqrt{\Delta\mathfrak{S}^2(\delta, \Delta\delta; \lambda) + \overline{\mathfrak{C}}^2(\delta, \Delta\delta; \lambda)} = |\kappa_c|T \tag{12a}$$

$$\tan^{-1}\frac{\Delta\mathfrak{S}(\delta, \Delta\delta; \lambda)}{\overline{\mathfrak{C}}(\delta, \Delta\delta; \lambda)} = \Delta\delta - \Delta\phi \tag{12b}$$

Equation (12) allow us solving feasible $\Delta\delta$ and κ_c when δ, $\Delta\phi$ and λ are given.

The precise solution of $\Delta\delta$ can be obtained from (12b) with Newton's method since κ_c does not participate in this equation. Then, once the feasible $\Delta\delta$ is calculated, κ_c can be directly calculated with (12a). After that, with the known λ, δ_0, δ_1 and κ_c, all the rest parameters can be obtained.

The tuning method for the symmetric elementary path is also available for the unsymmetric one, shown in Fig. 5. The simplest solution is to adjust λ directly. Whenever λ is updated, the whole curve can be refreshed with (12). It is important to note that, according to (10), the lower bound of the adjustment range of λ is no longer be 0, but

$$\lambda_{\min} \triangleq \tan_{\mathcal{E}}^{-1}\left\{2\delta; \tan\left[\delta + \mathrm{sgn}(\delta)|\Delta\phi|\right]\right\}.$$

Next, the tuning method based on κ_c is considered. Finding the corresponding λ and $\Delta\delta$ to κ_c implies fully solving the nonlinear system (11), which can be achieved with 2D Newton's

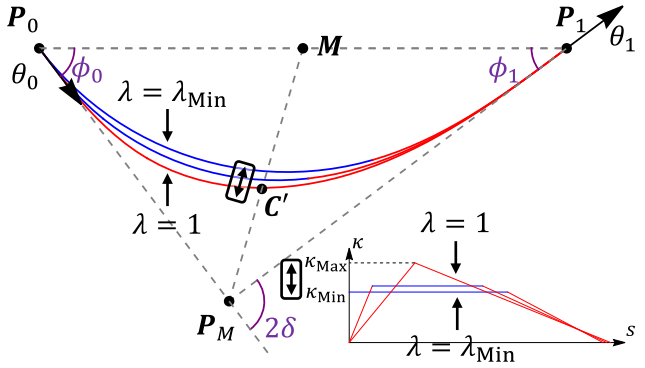

Fig. 5. Different unsymmetric elementary paths in the same enveloping triangle with multiple tuning methods presented.

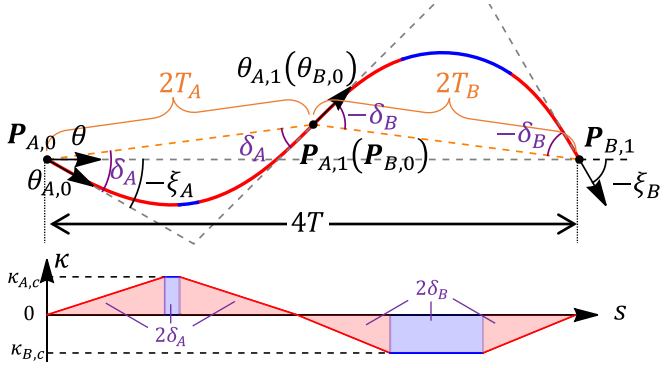

Fig. 6. A dual elementary path for lane changing cases.

method. The Jacobian matrix used in the method can quickly build from (5). The initial solution of $\Delta\delta$ is set to 0, while the initial solution of λ is calculated with (8) since it corresponds to the symmetric cases.

Finally, the tuning method via a special point is analyzed. Unfortunately, the connection point $\mathbf{C}$ in an unsymmetric case has a complex trail when λ changes. For instance, when $\lambda \to \lambda_{\min}$, $\mathbf{C}$ will move toward one of the boundary points. This problem makes $\mathbf{C}$ unsuitable for a control point.

The intersection point $\mathbf{C}'$ between the midline $\overline{\mathbf{MP}_M}$ and the unsymmetric elementary path is selected as the control point. $\mathbf{C}'$ has the similar properties to $\mathbf{C}$ in the symmetric cases. Meanwhile, when $\Delta\phi \to 0$, $\mathbf{C}'$ will degenerate to $\mathbf{C}$.

Assuming n is the directed length of $\overrightarrow{\mathbf{C}'\mathbf{M}}$, an expression similar to (9) holds, which is

$$\eta_n \triangleq \frac{n}{N} = \frac{\tan_{\mathcal{E}}(\delta;\lambda)}{\tan\delta}\gamma(\delta,\Delta\phi;\lambda). \tag{13}$$

γ is an empirical formula, which is

$$\gamma(\delta,\Delta\phi;\lambda) \approx \cos\left\{\frac{\Delta\phi}{\delta}\left[\frac{\pi}{2}-(1-\lambda)^2\right]\right\}$$

For any fixed η_n, the corresponding λ can be solved with (13) by Newton's method. Thus, the unsymmetric elementary path can be tuned by moving $\mathbf{C}'$ on $\overline{\mathbf{MP}_M}$.

VI. Dual Elementary Path

If θ_0 and θ_1 lay on the same side of $\overrightarrow{\mathbf{P}_0\mathbf{P}_1}$, multiple elementary paths are required. These boundary conditions are common in lane change scenarios. According to [9], [10], two connected elementary paths are enough to solve them.

As shown in Fig. 6, the two elementary paths are distinguished with the subscript "A" and "B". The known boundary conditions are $\{\mathbf{P}_{A,0},\theta_{A,0}\}$ and $\{\mathbf{P}_{B,1},\theta_{B,1}\}$ respectively, and the G^2 continuity at the connection point leads to

$$\mathbf{P}_{A,1} = \mathbf{P}_{B,0},\ \theta_{A,1} = \theta_{B,0}$$

Similar to the previous analysis, the boundary conditions are translated into auxiliary variables $\{\xi_A,\xi_B,T\}$ to avoid the absolute positions and orientations, which are

$$\xi_A \triangleq \theta_{A,0}-\theta,\ \xi_B \triangleq \theta_{B,0}-\theta,\ T \triangleq \frac{1}{4}\|\mathbf{P}_{A,0}\mathbf{P}_{B,1}\|,$$

and θ is the corresponding orientation for $\overrightarrow{\mathbf{P}_{A,0}\mathbf{P}_{B,1}}$. ξ_A and ξ_B can further transform into

$$\bar{\xi} \triangleq \frac{1}{2}(\xi_A+\xi_B),\ \Delta\xi \triangleq \frac{1}{2}(\xi_A-\xi_B). \tag{14}$$

Next, the orientation relationship $\xi_A + 2\delta_A + 2\delta_B = \xi_B$ allows us using a single auxiliary variable $\bar{\delta}$ to represent δ_A and δ_B, which are

$$\delta_A = \bar{\delta} - \frac{\Delta\xi}{2},\ \delta_B = -\bar{\delta} - \frac{\Delta\xi}{2}. \tag{15}$$

The original interpolation problem has up to 5 ° of freedom. 3 of them are the arbitrariness of selecting the connecting states, while the other 2 lead to the adjustment of each elementary path in fixed enveloping triangles. This section introduces several extra constraints to quickly find a simple and feasible solution.

The first two constraints are chosen naturally, where the two elementary paths are required to be symmetric. Under these constraints, the geometric relationship leads to

$$2T_A\begin{pmatrix}\cos(\xi_A+\delta_A)\\ \sin(\xi_A+\delta_A)\end{pmatrix} + 2T_B\begin{pmatrix}\cos(\xi_A+2\delta_A+\delta_B)\\ \sin(\xi_A+2\delta_A+\delta_B)\end{pmatrix} = \begin{pmatrix}4T\\0\end{pmatrix}.$$

With (14) and (15), it can be simplified to

$$\tan(\bar{\delta}+\bar{\xi}) = \frac{T_b-T_a}{T_b+T_a}\tan\frac{\Delta\xi}{2} \tag{16a}$$

$$4T^2 = T_a^2 + 2T_aT_b\cos\Delta\xi + T_b^2 \tag{16b}$$

The third constraint is designed to satisfy (16a), which is $T_A = T_B$, or equivalent to $\bar{\delta}+\bar{\xi}=0$. This constraint also indicate $\mathbf{P}_{A,1}$ laying on the perpendicular of $\mathbf{P}_{A,0}\mathbf{P}_{B,1}$, which is same to that in [9]. Under the three extra constraints, the parameters of both elementary paths can be solved as

$$T_A = T_B = \frac{T}{\cos\frac{\Delta\xi}{2}},\ \delta_A = -\bar{\xi}-\frac{\Delta\xi}{2},\ \delta_B = \bar{\xi}-\frac{\Delta\xi}{2} \tag{17}$$

With (17), the enveloping triangle of the two elementary paths can be uniquely determined. Then, the two paths can be tuned with any methods in Section V.

Some of the special situations are investigated. First, when $\lambda_A = \lambda_B = 1$, the proposed method degenerates to that in [9], where the whole path is composed of clothoid segments. Then, when $\Delta\xi = 0$, which is a typical case in paralleled parking and lane changing, the proposed method degenerates to that in [2].

TABLE I
ELEMENTARY PATH EVALUATION RESULT

Conditions	Sym. Path			Unsym. Path			
	λ	κ_c	n	Term	λ	κ_c	n
Max Rel. Err. ($\times 10^{-4}$)	/	0.003	0.11	0.005	/	0.005	109.7
Avg Rel. Err. ($\times 10^{-6}$)	/	0.007	0.05	0.004	/	0.014	3582
Avg. Time (μs)	5.4	17.6	32.8	/	49.2	98.0	100.8
Avg. Time for [1] (μs)	SM	18.0	✗	/	33.7*	✗	✗
Avg. Time for [2] (μs)	SM	20.7	✗	/	✗	✗	✗
Avg. Time for [3] (μs)	984*	✗	✗	/	9696*	✗	✗

SM: Same non-iterative method. *: Only valid for $\lambda = 1$. ✗: Unsupported.

Finally, when λ_A and λ_B are tuned to satisfy $\kappa_{A,c} = \kappa_{B,c}$, the generated result will be similar to that in Tian's method [10].

VII. EXPERIMENTS

Various experiments are carried out to verify the proposed method's extreme generalizability and efficiency while revealing its high flexibility for usage in global planning, HD map generation, and highway design. Moreover, compared with the widely used interpolation curve like Bézier curve and B-spline curve, the proposed method has better control of the curvature profile.

The performance of the proposed method is verified by finding feasible solutions for different boundary conditions. For each case, the boundary conditions include the position and the orientation of the two terminal states, and one of λ, κ_c or n condition. The boundary conditions are extracted from the randomly generated elementary paths to ensure a feasible solution exists. The verification is performed randomly for 10^5 times, and the results are summarized in Table I.

The accuracy of the proposed method is measured with the relative error between the properties of the generated curve and the corresponding condition. For some of the boundary conditions, the error does not exist by definition, like the error on boundary orientation or the error on λ. Moreover, the position error on the boundary states only exists for the unsymmetric cases. This is evaluated by the Euclidean distance between the terminal point of the generated path and the given constraints while being normalized with the parameter T. The relative terminal error is marked as "Term" in the table and is calculated with the λ condition input. Since λ also acts as the intermediate variable in other boundary conditions, they have the same terminal error results.

The efficiency of the proposed method is measured with the average time consumption of a single calculation on a Python-based implementation. Moreover, it does not include the time for case generation and validation.

According to the result in the table, even in the most complex situation, the unsymmetric elementary path with given n, the relative error on n is no more than 1.1%, and the time consumption is about 0.1 ms. Meanwhile, all other errors and time consumption are almost negligible. This result shows the high efficiency and generalizability of the proposed method for any boundary condition, making it highly available in planning scenarios with high-frequency calculations.

Three state-of-the-art elementary path generation methods are introduced for comparison, which are Walton's method [1], Wilde's method [2] and pCCP path [3], respectively. The first two use Newton's method to find the solution, while the last one uses the bisection method. These methods are tuned to reach the same average error level as the proposed method, and the corresponding time consumptions are recorded. For the cases with given λ, the same average error level on the terminal state is required.

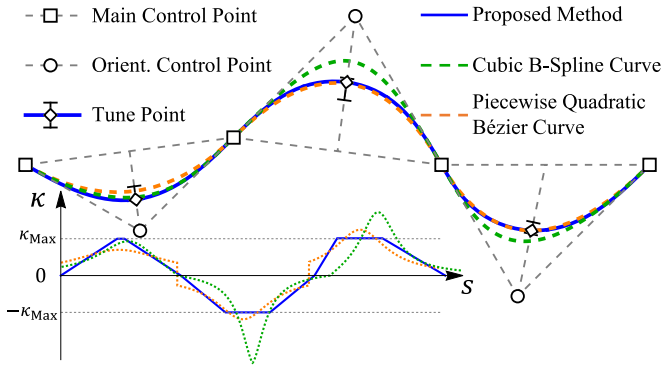

Fig. 7. Controllable path manipulation. The path is composed of multiple elementary paths. The quadratic Bézier curve and cubic B-spline curve under the same control input are used for comparison, where the proposed method has a higher controllability over the curve's shape and curvature profile.

The two related works with Newton's method are first considered. For the symmetric case, the performances of these methods are almost identical. When λ is provided, the expression of these methods is totally the same, while when κ_c is provided, the residual expressions of these methods are also equivalent to each other. However, the proposed method is the only method that can find a feasible solution with n. Next, the proposed method reveals greater advantages for the unsymmetric cases since it is the only method that can adopt different types of boundary conditions. As a comparison, only Walton's method can find a feasible solution under $\lambda = 1$.[1] Note that [1] has a lower time consumption than the proposed method. This is because the residual function used in [1] has better linearity characteristics than (12b). However, their residual function cannot be generalized to the cases with smaller λ, or cases with other constraints.

Compared with Newton's method, the bisection-based method is much slower. In the pCCP method [3], a 2D bisection method is used for searching, which makes its time consumption hundreds of times more than the proposed method, thus significantly limiting its application.

The rest of the section shows the flexibility of the proposed method for HD map editing and highway shape design tasks, which require long smooth path generation with editable control points. This purpose can be achieved by connecting multiple elementary paths in a spline-liked form. The whole path is initialized with a set of control points with orientations, which are used to generate enveloping triangles. If two adjacent control points do not meet the requirements, a new control point can insert between them according to Section VI as the initial solution. An illustrative example of the whole path with the control points is shown in Fig. 7.

After the initialization of the path, the modification of it can also be done naturally. Like other control points-based splines,

[1] In [1], one can get unsymmetric results with smaller λ by given $\lambda\delta_0$. However, this is not a natural way to edit the curve, while there are no corresponding conditions in the proposed method.

the generated path can be modified by moving and rotating the control points (shown as the hollow squares and circles in Fig. 7), which act on the shape of each enveloping triangle. Besides, the shape of each elementary path can also be tuned by moving the controllable midpoint (shown as the hollow diamonds in the figure). Moreover, these modifications can be performed locally since moving the midpoints won't affect other parts. The above properties allow us to build a friendly human-computer interface for creating and editing the long path. An interactive illustrational example is open-sourced in https://github.com/ZhangSongyi/clothoid_arc_turn, while the demonstration can be seen in the attached video.

Finally, the proposed method is compared with other commonly used interpolation curves in map editing. The compared curves are the piecewise quadratic Bézier curve and the cubic B-spline curve, respectively, since they can be uniquely determined with the same control point input as the proposed method. The comparison result is shown in Fig. 7. According to the comparison of the curvature profile, the piecewise quadratic Bézier curve cannot satisfy G^2-continuity at the control points. Meanwhile, the cubic B-spline sometimes generates higher curvature and curvature change rates than the proposed method. The only way to optimize these curves' curvature profile is to increase the curve's order, like piecewise quartic B-spline, piecewise cubic Bézier curve, etc. However, the higher degree of freedom also brings more control points, which do not have a simple relationship to curvature, therefore, cannot be tuned intuitively. As a comparison, adopting the proposed method gives us higher controllability over the curve's shape and curvature profile.

VIII. Conclusion

This letter presents a novel method for evaluating and tuning clothoid-based elementary paths with multiple types of boundary constraints. The generated path can G^2-continuously connect states with null curvature, meanwhile being fine-tuned with both maximum curvature and the midpoint's position. Such properties make it highly acceptable in local planning, highway design and HD-map editing. Various experiments show that the proposed method achieves higher robustness, efficiency and flexibility than the existing methods.

References

[1] D. J. Walton and D. S. Meek, "A controlled clothoid spline," *Comput. Graph.*, vol. 29, no. 3, pp. 353–363, 2005.

[2] D. K. Wilde, "Computing clothoid segments for trajectory generation," in *Proc. IEEE/RSJ Int. Conf. Intell. Robots Syst.*, 2009, pp. 2440–2445.

[3] S. Gim, L. Adouane, S. Lee, and J.-P. Derutin, "Clothoids composition method for smooth path generation of car-like vehicle navigation," *J. Intell. Robotic Syst.*, vol. 88, pp. 129–146, 2017.

[4] S. Zhang, Z. Jian, X. Deng, S. Chen, Z. Nan, and N. Zheng, "Hierarchical motion planning for autonomous driving in large-scale complex scenarios," *IEEE Trans. Intell. Transp. Syst.*, vol. 23, no. 8, pp. 13291–13305, Aug. 2022.

[5] J. Pang, S. Zhang, J. Fu, J. Liu, and N. Zheng, "Curvature continuous path planning with reverse searching for efficient and precise autonomous parking," in *Proc. IEEE 25th Int. Conf. Intell. Transp. Syst.*, 2022, pp. 2798–2805.

[6] D. Kiss and G. Tevesz, "Autonomous path planning for road vehicles in narrow environments: An efficient continuous curvature approach," *J. Adv. Transp.*, vol. 2017, 2017, Art. no. ID-2521638.

[7] T. Fraichard and A. Scheuer, "From Reeds and Shepp's to continuous-curvature paths," *IEEE Trans. Robot.*, vol. 20, no. 6, pp. 1025–1035, Dec. 2004.

[8] J. Funke et al., "Up to the limits: Autonomous Audi TTS," in *Proc. IEEE Intell. Veh. Symp.*, 2012, pp. 541–547.

[9] J. A. R. d. Silva, "Piecewise linear continuous-curvature path planning for autonomous vehicles," Ph.D. dissertation, Universidade de São Paulo, São Paulo, Brazil, 2018.

[10] Y. Tian, Z. Chen, C. Xue, Y. Sun, and B. Liang, "Continuous curvature turns based method for least maximum curvature path generation of autonomous vehicle," in *Proc. IECON 47th Annu. Conf. IEEE Indust. Electron. Soc.*, 2021, pp. 1–6.

[11] S. Gim, L. Adouane, S. Lee, and J.-P. Derutin, "Parametric continuous curvature path for smooth steering with car-like vehicles," in *Intell. Auton. Syst. 13: Proc. 13th Int. Conf.*, 2015, pp. 1327–1342.

[12] E. Bertolazzi and M. Frego, "Interpolating clothoid splines with curvature continuity," *Math. Methods Appl. Sci.*, vol. 41, no. 4, pp. 1723–1737, 2018.

[13] E. D. Lambert, R. Romano, and D. Watling, "Optimal smooth paths based on clothoids for car-like vehicles in the presence of obstacles," *Int. J. Control, Automat. Syst.*, vol. 19, pp. 2163–2182, 2021.

[14] T. Officials, *A Policy on Geometric Design of Highways and Streets*. Washington, D.C, USA: AASHTO, 2011.

[15] M. Dupuis, M. Strobl, and H. Grezlikowski, "Opendrive 2010 and beyond–status and future of the de facto standard for the description of road networks," in *Proc. Driving Simul. Conf. Eur.*, 2010, pp. 231–242.

[16] Y. Zhou, R. Huang, T. Jiang, Z. Dong, and B. Yang, "Highway alignments extraction and 3D modeling from airborne laser scanning point clouds," *Int. J. Appl. Earth Observ. Geoinformation*, vol. 102, 2021, Art. no. 102429.

[17] M. A. Heald, "Rational approximations for the Fresnel integrals," *Math. Computation*, vol. 44, no. 170, pp. 459–461, 1985.